JOURNAL OF MATERIALS SCIENCE **34** (1999) 1885–1897

The creep behaviour of isotropic polyethylene

M. BONNER, R. A. DUCKETT, I. M. WARD
IRC in Polymer Science and Technology, The University of Leeds, Leeds, LS2 9JT, UK
E-mail: i.m.ward@leeds.ac.uk

Dead loading creep and constant strain rate yield experiments have been used to study the tensile creep behaviour of three grades of isotropic polyethylene. This has provided further evidence for the existence of two yield points in isotropic polyethylene. Two different models have been used to attempt to describe this behaviour. Although the results can be described by to both the two process model of Wilding and Ward and the co-operative jump model of Fotheringham and Cherry, it appears that the two process model provides a more convincing quantitative fit to the data.

1. Introduction

In recent years research has been performed on the yield behaviour of isotropic polyethylenes [1–3], in particular into the existence of two yield points in these materials [1]. A Fotheringham and Cherry analysis [3, 4] has been used successfully to describe this behaviour in terms of a co-operative jumps over an energy barrier. The research reported in this paper extends the previous work by showing evidence for yield points in tensile creep experiments in addition to the previously reported constant strain-rate tests [1]. A model originally proposed by Wilding and Ward [5] to describe the tensile creep behaviour of highly oriented polyethylene in terms of two Eyring processes acting in parallel has also been successfully used to describe the behaviour of the isotropic material. The Fotheringham and Cherry model has been shown to produce parameters which are extremely dependent upon the constraints placed on the parameters and the interpretation of the recovery stress.

2. Experimental

2.1. Materials used

This investigation concerns the behaviour of isotropic samples of three grades of polyethylene, whose physical characteristics are shown in Table I. Of these grades B and D are medium density copolymers with different concentrations of butyl branches, while C is a linear high density homopolymer. Density was measured on quenched compression moulded sheets using a standard density column at 20 °C.

2.2. Sample preparation

Samples for testing were produced from compression moulded sheets. These sheets were prepared by placing a known quantity of the polymer pellets between polished brass plates. These plates were then placed between the platens of a hot press heated to 160 °C, and contact pressure was applied. After the temperature had stabilised, a load of 20 tons on a four inch diameter ram (equal to 2.1 MPa on the brass plates), was applied. This load was held for 5 min before the plates were cooled. Cooling was achieved either by quenching, in which the plates were cooled from 160 °C by placing them in water at room temperature, or by slow cooling, in which the platens of the press were cooled at a controlled rate of 2 °C/min. The sheets were approximately 30 cm in diameter and between 0.1 and 0.3 mm thick. The two different cooling treatments produced radically different initial morphologies, as can be seen from the crystallinity measurements in Table II. These were derived by DSC experiments on samples from the compression moulded sheets.

Samples for mechanical tests were then cut from these sheets using dumbbell cutters. Two cutters were used. One had a parallel sided section 16 mm in length the other had a parallel sided section 81 mm in length. Both parallel sided sections were 2 mm wide.

2.3. Mechanical tests

2.3.1. Creep

Creep tests were performed using a dead loading creep apparatus as described in [6]. The sample was mounted vertically and known masses were used to apply load at the bottom end. A linear displacement transducer was used to monitor displacement at this point. Although gauge lengths varied slightly, a minimum gauge length of 70 mm was used and the actual gauge length was recorded to ±0.2 mm. The supporting apparatus had a deflection of less than 0.14 mm when using a load of less than 2.5 kg, and the highest load applied in this work was 2 kg. The sample slipped slightly in the grips when the load was applied, the amount of slippage was variable, the maximum observed was 0.25 mm when using a trial 2.5 kg load on a 70 mm gauge length sample. This is important since the samples were not conditioned. The output of the transducer was monitored by a PC, using a programme which automatically recorded the times at which each increment in nominal

TABLE I Physical characteristics of the grades of polyethylene studied

Grade	$\bar{M}_W$	$\bar{M}_N$	Branch content (per 1000 carbons)	Density (Quenched)
B	206,000	12,900	6.2	932.6 kg m^{-3}
C	131,000	19,100	less than 0.1	947.1 kg m^{-3}
D	156,000	17,000	1 to 2	943.1 kg m^{-3}

TABLE II Yield stress, natural draw ratio and crystallinity for the three grades of polyethylene studied

Grade	Yield stress (MPa)	Natural draw ratio	Percentage crystallinity	Creep performance
Slow cooled C	30.7 ± 0.1	10.5 ± 0.5	77.2 ± 1.5	1
Slow cooled D	28.3 ± 0.2	9.1 ± 0.5	68.4 ± 1.4	2
Quenched C	21.3 ± 0.3	8.4 ± 0.5	64.3 ± 1.3	3
Quenched D	19.5 ± 0.4	6.8 ± 0.3	60.1 ± 1.2	4
Slow cooled B	17.1 ± 0.3	6.4 ± 0.3	54.6 ± 1.1	5
Quenched B	14.9 ± 0.2	5.2 ± 0.3	49.2 ± 1.0	6

strain of 0.2% occurred. The recorded strain/time data were analysed in a spreadsheet application using an approximation method to obtain the true strain rate at any required strain. The experiments were monitored until the sample formed a neck and began to deform inhomogeneously. The strain at which this occurred varied between 15 and 60% depending upon the material used and the conditions of the test.

The creep rigs were housed in a temperature controlled laboratory, where the temperature was maintained at 20 °C to within 2 deg. Also one creep rig was equipped with an environmental chamber to work at elevated temperatures. Heating was achieved by passing compressed air over a heating coil before it entered the chamber. The temperature could be maintained to better than 0.5 °C above 30 °C. Elevated temperature tests were performed between 30 and 70 °C, most especially at 50 and 70 °C. Room temperature tests were performed without the chamber at 20 °C.

2.3.2. Yield stress

These tests were conducted on an Instron tensile testing machine. The samples (with gauge lengths of 81 mm), were mounted between clamps and the crosshead speed selected to give the required initial strain rate. The yield stress was determined from the output of the load cell at its peak value and dividing by the true cross sectional area of the sample (which was calculated from the measured initial cross sectional area assuming the sample maintained a constant volume).

2.3.3. Transient stress dip tests

These were performed using the method of Fotheringham and Cherry [1, 4], and involved first straining a sample and then immediately removing some of the applied strain and allowing the load to relax at constant strain.

Test specimens were loaded into an Instron and the crosshead speed was selected and movement of the crosshead started. When the sample had reached a predetermined value of strain, ε_1, the crosshead was reversed at five times its forward speed for a known distance and then brought to rest at a strain level of ε_2; a fresh sample was used for each experiment.

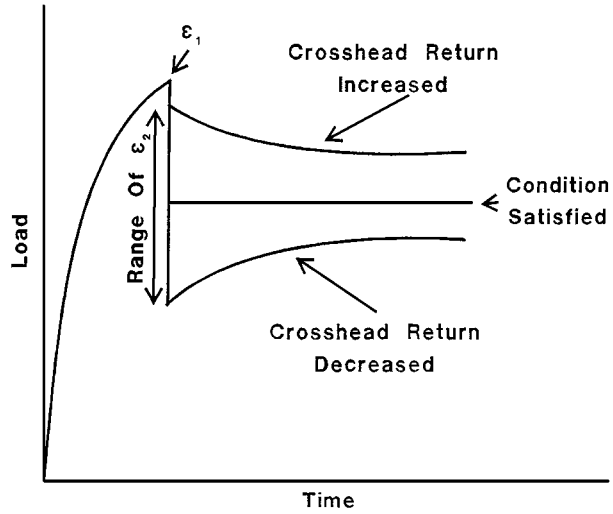

Figure 1 Crosshead return protocol for transient stress dip tests.

The output from the load cell was observed whilst the strain in the sample was held constant at ε_2. The tests involved searching for the value of ε_2 for each ε_1 at which the load output remained constant with time. A schematic representation of the load output against time (see Section 4), and the necessary corrections to the return distance of the crosshead are shown in Fig. 1.

3. Results

3.1. General creep performance

The data collected from the creep apparatus described earlier were transferred to a spreadsheet and plotted after the manner of Sherby and Dorn [7], that is as $\log_{10}$ (strain rate) versus strain at constant nominal stress. Sherby Dorn plots for materials B, C and D in the quenched state are shown in Figs 2 to 4 respectively.

In this work we have graded the creep performance of the material according to its creep strain rate at a given stress and strain. In order for this ranking to be meaningful the strain level set must be greater than the strain at which the first yield point is encountered and below the strain at which the second yield point occurs. If this condition is observed then we believe that we are measuring a unique strain rate which is dependent solely upon the stress and strain level of the material (see Section 3.3). Thus in this work a material performs better if it exhibits a lower creep strain rate than another material at the same levels of stress and strain. Using this definition it can be seen that material C has the best creep performance, B the worst creep performance, whilst D is intermediate between the two. This behaviour correlates with the crystallinity of the material, the increased crystallinity of material C being associated with its good creep performance. Indeed in both the quenched and slow cooled morphologies both

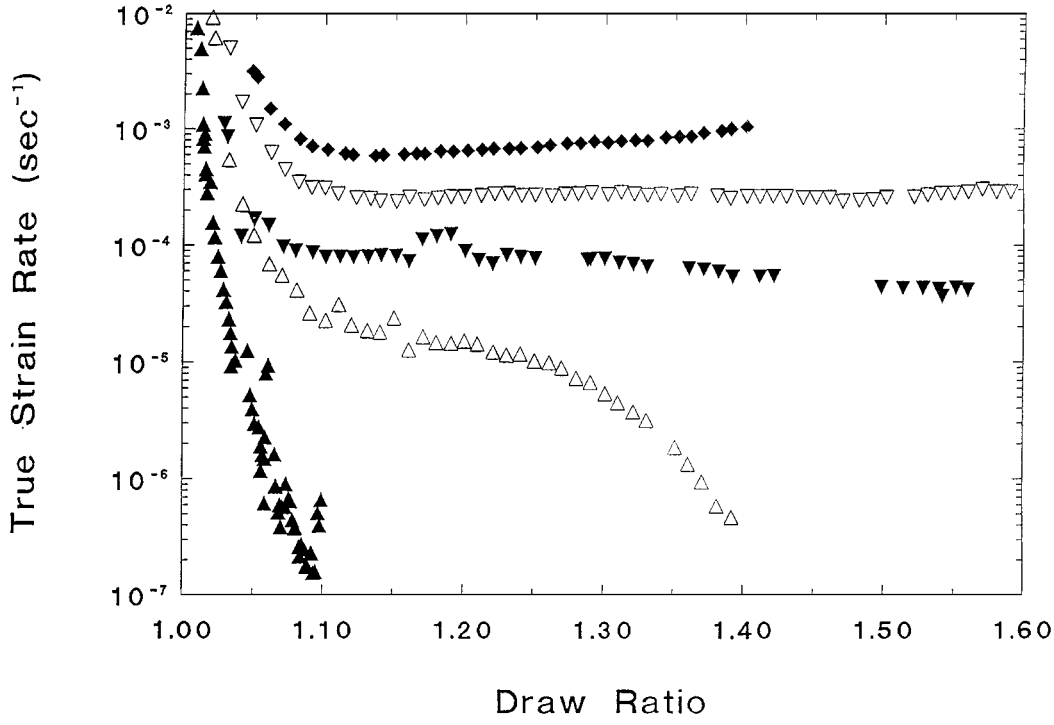

Figure 2 Sherby Dorn plots for the quenched morphology of grade B at 20 °C, at nominal stress levels of, ▲ 7.3 MPa, △ 9.3 MPa, ▼ 11.3 MPa, ▽ 12.0 MPa, ◆ 12.5 MPa.

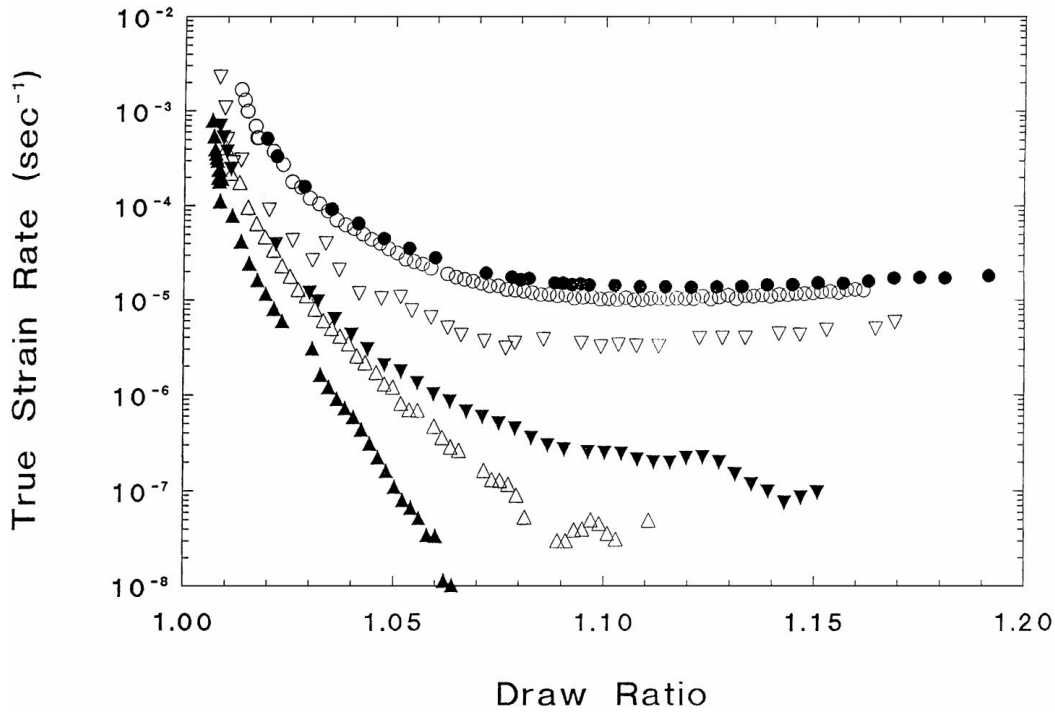

Figure 3 Sherby Dorn plots for the quenched morphology of grade C at 20 °C, at nominal stress levels of, ▲ 8.5 MPa, △ 10.0 MPa, ▼ 10.5 MPa, ▽ 11.1 MPa, ○ 12.8 MPa, ● 13.5 MPa.

the creep performance rating and the yield stress rank with the crystallinity. The values of percentage crystallinity, yield stress (at a true strain rate of 0.005 s^{-1}), and creep performance ranking (the best creep performance being ranked as 1, the worst as 6), are given in Table II.

Table II also shows that the slow cooled morphologies of each material have better creep performance than the quenched material. This is shown graphically in Figs 5 to 7. In these figures quenched and slow cooled samples were loaded at equal nominal stresses. The results indicate at least an order of magnitude decrease in strain rate in the slow cooled compared with the quenched material. This indicates a major change of creep response resulting from changes in the morphology of the material. However Figs 6 and 7 also show that if the increased yield stress of the slow cooled material is taken into account the creep performance is essentially the same. In order to take the higher yield stress into account the yield stress was measured for

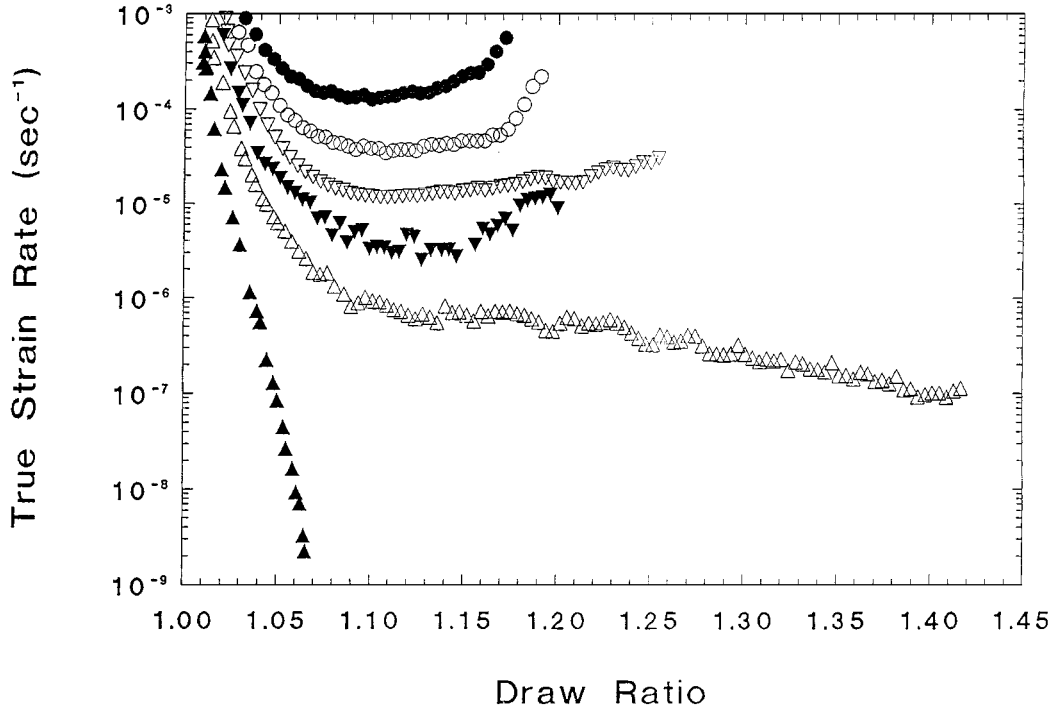

Figure 4 Sherby Dorn plots for the quenched morphology of grade D at 20 °C, at nominal stress levels of, ▲ 8.0 MPa, △ 10.0 MPa, ▼ 11.1 MPa, ▽ 12.0 MPa, ○ 13.0 MPa, ● 14.0 MPa.

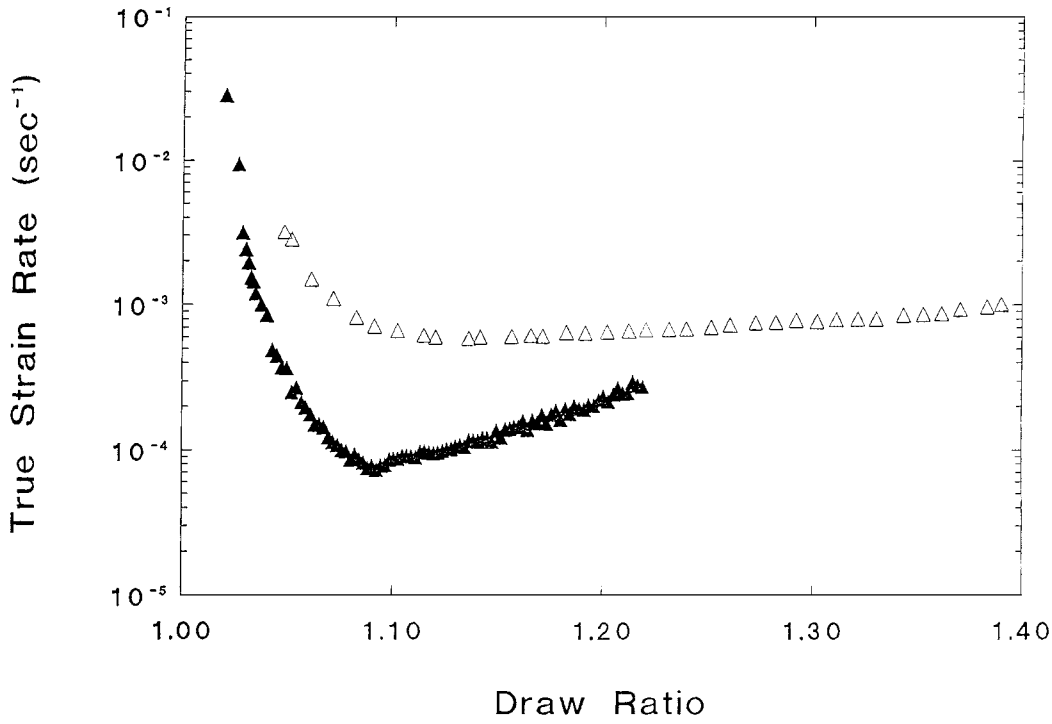

Figure 5 Sherby Dorn plots showing the difference in creep performance between the quenched (△) and slow cooled (▲) morphologies of grade B at 20 °C and 12.5 MPa.

both the quenched and slow cooled morphologies at a true strain rate of 0.005 s^{-1}, and then creep tests were performed so that the stress used in the test was a fixed percentage of the yield stress of the material (60% for grade C, 67% for grade D).

Taken together these results indicate that the crystallinity of the material plays an important role in determining the creep performance, yield stress and natural draw ratio of the material, at least in the types of materials covered by this work.

3.2. Double yield points in polyethylene

Previous work by Brooks *et al.* [1] has provided evidence for the existence of two yield points in materials B and C. In this work samples of B and C were loaded at a constant nominal strain rate to different initial strains and the samples were then unloaded and allowed to recover for a period of three days and the amount of residual strain was measured. A graph of residual strain against applied strain was plotted (shown schematically in Fig. 8). The region with zero gradient at small strains

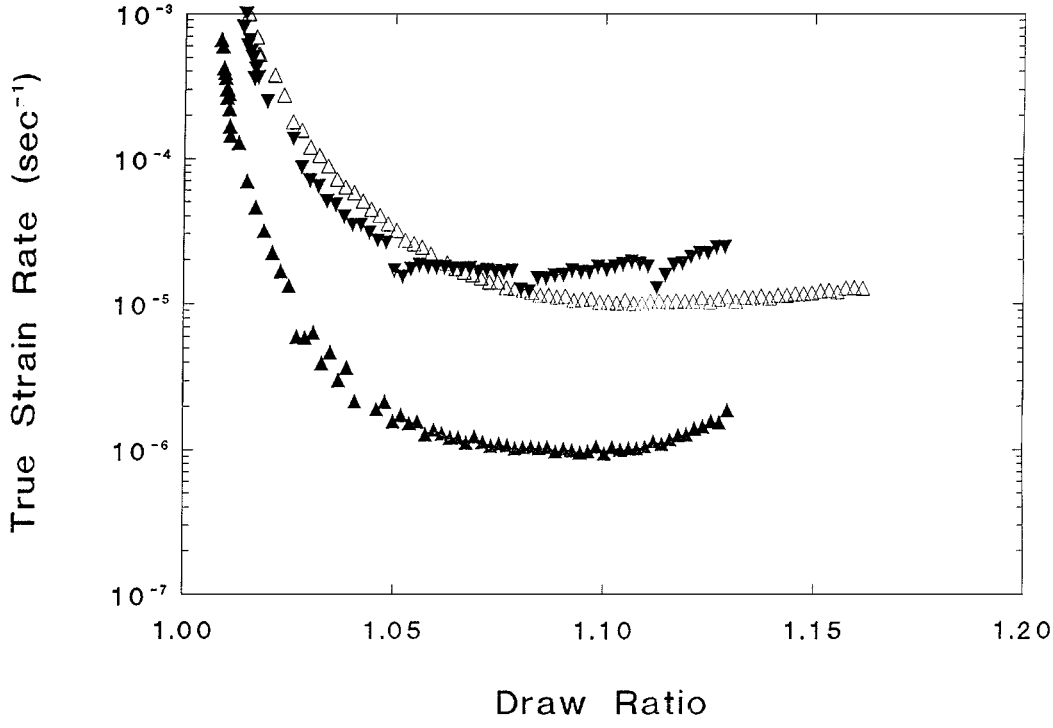

Figure 6 Sherby Dorn plots showing the difference in creep performance between the quenched and slow cooled morphologies of grade C at both equal stress and equal percentage of the yield stress at 20 °C. (△) quenched, 13 MPa, (▲) slow cooled, 13 MPa, (▼) slow cooled, 18.8 MPa.

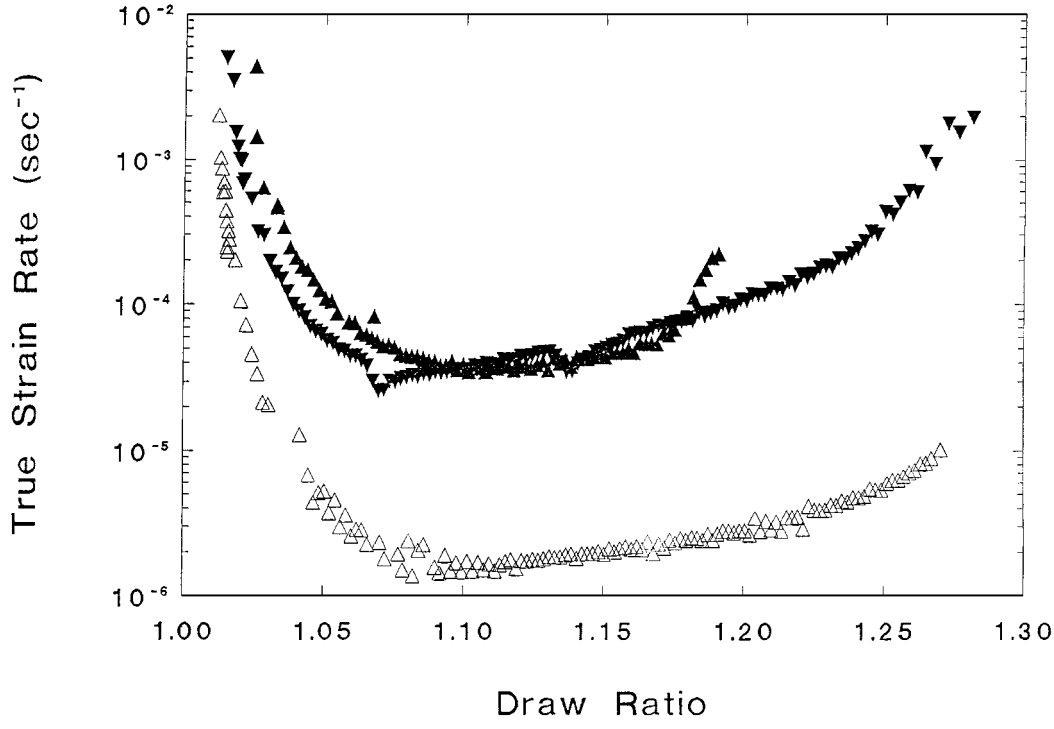

Figure 7 Sherby Dorn plots showing the difference in creep performance between the quenched and slow cooled morphologies of grade D at both equal stress and equal percentage of the yield stress at 20 °C. (△) slow cooled, 13 MPa, (▲) quenched, 13 MPa, (▼) slow cooled, 18.7 MPa.

indicates full, rapid recovery of the sample. The region at large strains with unit gradient indicates plastic, permanent deformation. The intermediate region indicates a state of partial recovery, and would not be present in a material with a single yield point.

The Sherby Dorn plots of Figs 2 to 7 also show evidence for two yield points. The first yield point is related to the transition of the Sherby Dorn plot from a rapid decrease in strain rate at low strains with strain to a region of lower slope, and occurs between 5 and 8% strain (similar to the transition reported by Brooks *et al.* [1]). This transition appears to be relatively independent of the material type. The second yield point is characterised in tension by a sharp necking of the sample to produce permanent plastic flow (also seen by Brooks *et al.*), and occurs between 15 and 40% depending on the material. Brooks *et al.* quote higher strain values for the second yield point, but as stated earlier worked

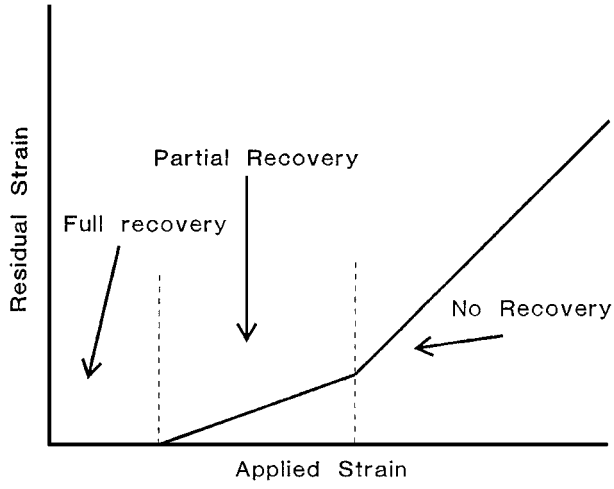

Figure 8 Schematic representation of the two yield point graph of Brooks *et al.*

predominantly in compression where the presence of flaws is less likely to produce stress concentrations which induce early necking. The manifestations of these two yield points on a typical Sherby Dorn plot are shown in Fig. 9.

3.3. Evidence for the existence of a unique stress, strain rate and strain relationship

The existence of a unique relationship between true stress, true strain rate and strain has been reported previously for various materials [8, 9] and for B, C and D in the oriented state [10]. This relationship is characterised by a surface in stress, strain, strain rate space, such that any combination of two of the three variables determines the third, no matter what path is used to reach the point. Thus plateau creep data should be the same as constant strain rate data derived from Instron yield tests. This is because at the maximum load (the classic yield point) in a constant strain rate test the strain rate of the testing machine exactly matches the plastic strain of the material. This yield point occurs before the material starts to neck, and so the stress, strain and strain rate data which is obtained up to that point is consistent with the data obtained from a creep test where the plastic strain rate is monitored. Fig. 10 shows both sets of data for the quenched morphology of grade C at 20 °C. As can be seen the agreement is excellent. Although more data is required in order to state categorically that this relationship holds for all the samples, these results indicate that it exists for initially isotropic samples of polymer C.

4. Modelling

The double yield point phenomena observed in this work may be thought of as a feature of the two process model by Wilding and Ward [5]. This can be interpreted mechanically as a system of two parallel arms, each composed of a spring in series with a highly non linear dashpot, as shown in Fig. 11. Each yield point is associated with the initial yielding of a single dashpot. At the first yield point the weak dashpot begins to flow; however as the strong dashpot has not begun to flow the strong spring is available to drive the system back towards zero strain when the stress is released. This accounts for the partial recovery seen for all strains beyond the first point. At the second yield point the strong dashpot begins to flow and all subsequent strain results in permanent plastic deformation.

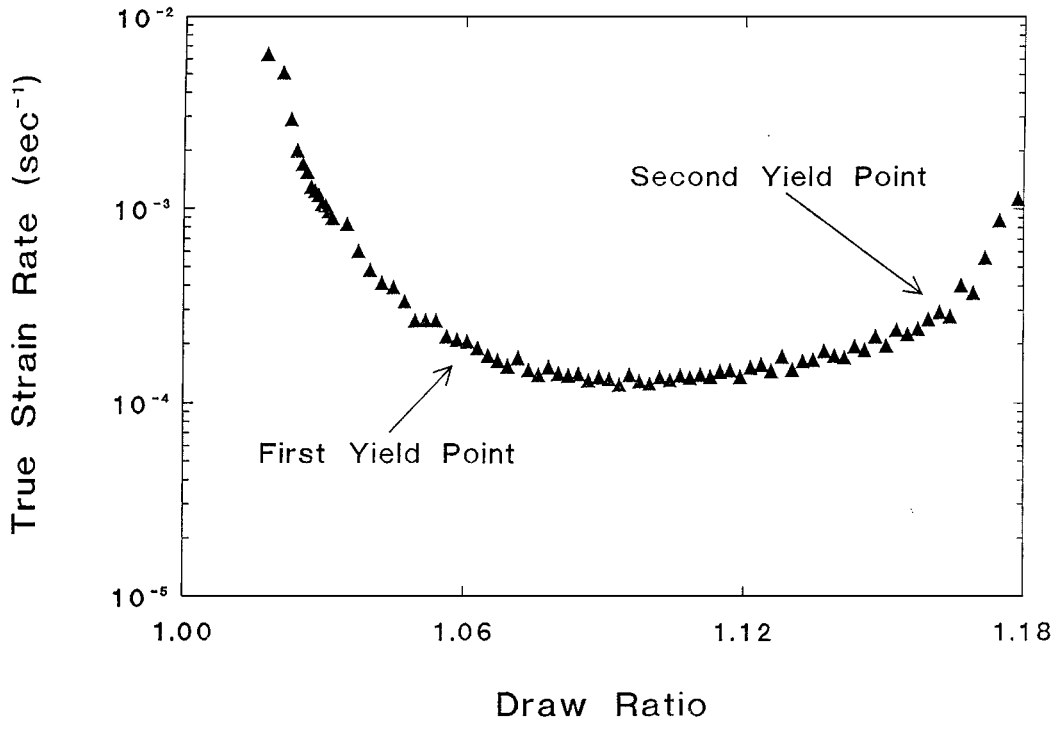

Figure 9 Sherby Dorn plot showing two yield points for the slow cooled morphology of grade B. For strains less than the 1st yield point recovery is complete within the machine resolution within 48 hours, for strains greater than the second yield point necking and permanent plastic flow is observed. At intermediate strains deformation is homogenous but recovery is not observed to approach the machine resolution within 7 days.

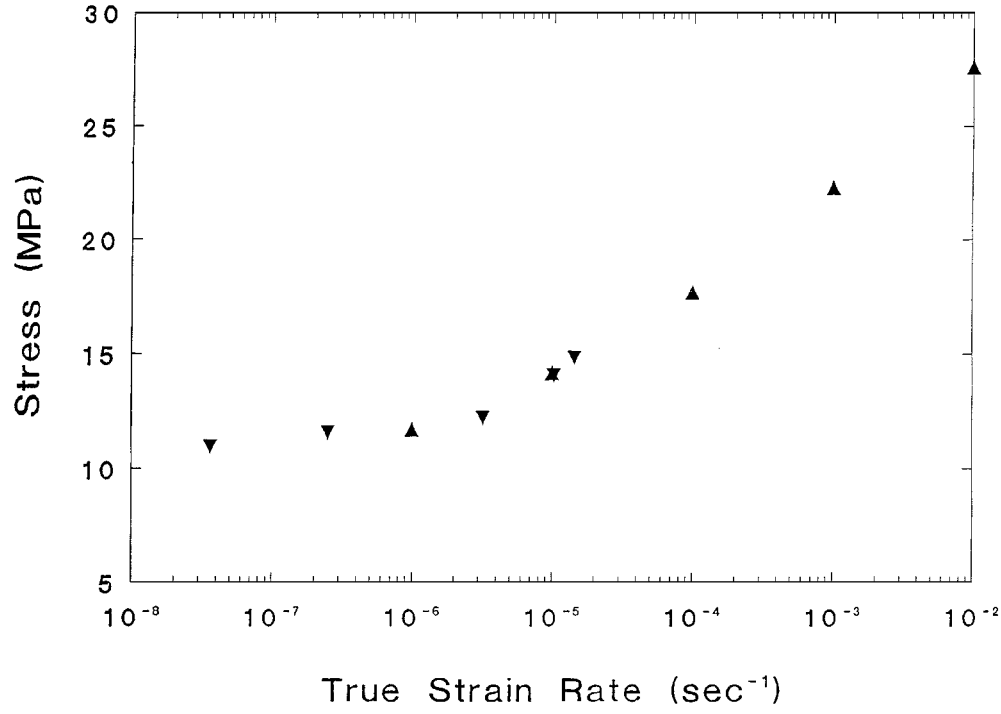

Figure 10 Plateau creep and Instron data for grade C at 20 °C, ▲ constant strain rate data, ▼ plateau creep data.

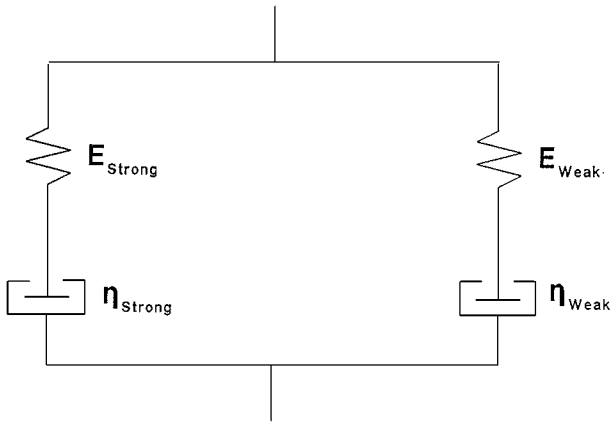

Figure 11 Schematic representation of the two process model.

If we assume that between the first and second yield points the strong dashpot does not flow, and hence has experienced no strain, then the model can be simplified by its removal. Thus we can use the transient stress dip tests of Fotheringham and Cherry [4] to determine the stress, σ_r, in the strong arm, which drives the recovery process. The weak dashpot carries a stress σ_e (the effective stress which drives the plastic deformation process), and the total stress applied to the system is σ_a. Hence

$$\sigma_e = \sigma_a - \sigma_r \tag{1}$$

After the strain dip when σ_a is above σ_r there is a positive stress on the dashpot, which subsequently decays when the dashpot flows. When σ_a is below σ_r the stress rises as the dashpot flows. If however σ_a is equal to σ_r there is no stress on the dashpot and hence there is no change in stress. By monitoring the behaviour of the stress over several experiments it is possible to determine σ_r and hence the stress in the strong arm for a known value of ε_1 the strain in each arm. Once the stress in the strong arm is known the modulus of the strong spring can be estimated, provided that we assume that it is Hookean, using

$$E = \frac{\sigma}{\varepsilon} \tag{2}$$

Knowing the modulus of the strong spring we can estimate the modulus of the weak spring. To do this we calculate the effective combined modulus of the two springs in the first few percent of the creep experiment, the quasi-linear region before any strain is taken up the dashpots, and then the weak modulus is easily defined since

$$E_{\text{combined}} = E_{\text{strong}} + E_{\text{weak}} \tag{3}$$

As can be seen from Table III the two modulus values are very similar.

4.1. Fitting to the two process model

It is possible to fit the plateau strain rate creep data for the quenched morphology of grade C at strain levels between the two yield points to the two process model of Wilding and Ward, which is described fully in [5]. In brief this model assumes that there are two processes active with increasing strain in the material,

TABLE III Modulus values of the weak and strong springs in the two process model

	Quenched C (MPa)	Quenched B (MPa)
E_{combined}	880	475
E_{strong}	425	250
E_{weak}	455	225

each of which carries a stress. At low stress levels the stress on one process dominates (denoted as process 1, the strong process), whilst the other process (process 2, the weak process), can dominate at high stress levels. It is assumed that both processes are described by the Eyring formulation [11], with process 1 (the strong process), always in the high stress approximation [5], as in Equation 4.

$$\sigma = \frac{2 \cdot 3kT}{V_{\text{strong}}}\left(\log_{10}(\dot{\varepsilon}) - \log_{10}\left(\frac{[\dot{\varepsilon}'_0]_{\text{strong}}}{2}\right)\right) + \frac{kT}{V_{\text{weak}}}\sinh^{-1}\left(\frac{\dot{\varepsilon}}{[\dot{\varepsilon}'_0]_{\text{weak}}}\right) \quad (4)$$

where

$$[\dot{\varepsilon}'_0]_n = \dot{\varepsilon}_{0n}\exp\left(\frac{-\Delta U_n}{kT}\right) \quad (5)$$

and $\dot{\varepsilon}$ is the rate of the activated process, $\dot{\varepsilon}_{0n}$ is a "pre exponential" factor, ΔU_n is the activation energy of the process, k is the Boltzmann constant, T is the temperature in Kelvin, σ is the applied stress, V_n is the activation volume of the process. In all cases n denotes which process (strong or weak), that the parameter is associated with.

The fitting procedure used was a least squares minimisation of the equation to the plateau creep data. All the four variables of Equation 4 (V_{strong}, V_{weak}, $[\dot{\varepsilon}'_0]_{\text{strong}}$, $[\dot{\varepsilon}'_0]_{\text{weak}}$), were allowed to vary to produce a free fit to the data. This fit is shown in Fig. 12, and the fitting parameters are shown in Table IV. As can be seen the fit is good, and the predicted strain rates for applied stresses of less than 10 MPa are very low. This is confirmed by ultra long term creep experiments which were unable to detect any plateau creep taking place at a stress level of 8 MPa.

TABLE IV Fitted parameters for the two process model fit for the quenched morphology of grade C

Parameter	Fitted value
V_1	14753 Å^3
V_2	2314 Å^3
$[\dot{\varepsilon}'_0]_1$	1×10^{-25}
$[\dot{\varepsilon}'_0]_2$	7.22×10^{-5}

Also by using a simplified method of Wilding and Ward [5] (where the overall material response at constant strain is split into high and low stress regions, each of which can be approximated by a single Eyring process), it is possible to derive an activation energy for both processes. This is done by measuring the creep rates at different temperatures for creep experiments at the same values of stress and strain. In this investigation the temperatures used were in the range 20 to 70 °C; higher temperatures could not be used since the material crept too fast to be monitored. When this was done the activation energies were measured to be 270 kJ mol^{-1} for the first (strong) process and 185 kJ mol^{-1} for the second (weak) process. Whilst the activation energy of the first process is still speculative due to the lack of sufficient data at low creep rates, the second process activation energy is better defined and is consistent with that obtained from dynamic mechanical measurements for the α relaxation which is generally considered to be a c-shear process [12, 13].

4.2. Fitting to the Fotheringham and Cherry model

Given the success of Brooks *et al.* [3] in using the Fotheringham and Cherry analysis to describe the behaviour of the quenched morphology of material B, it was decided to attempt to use the same model to

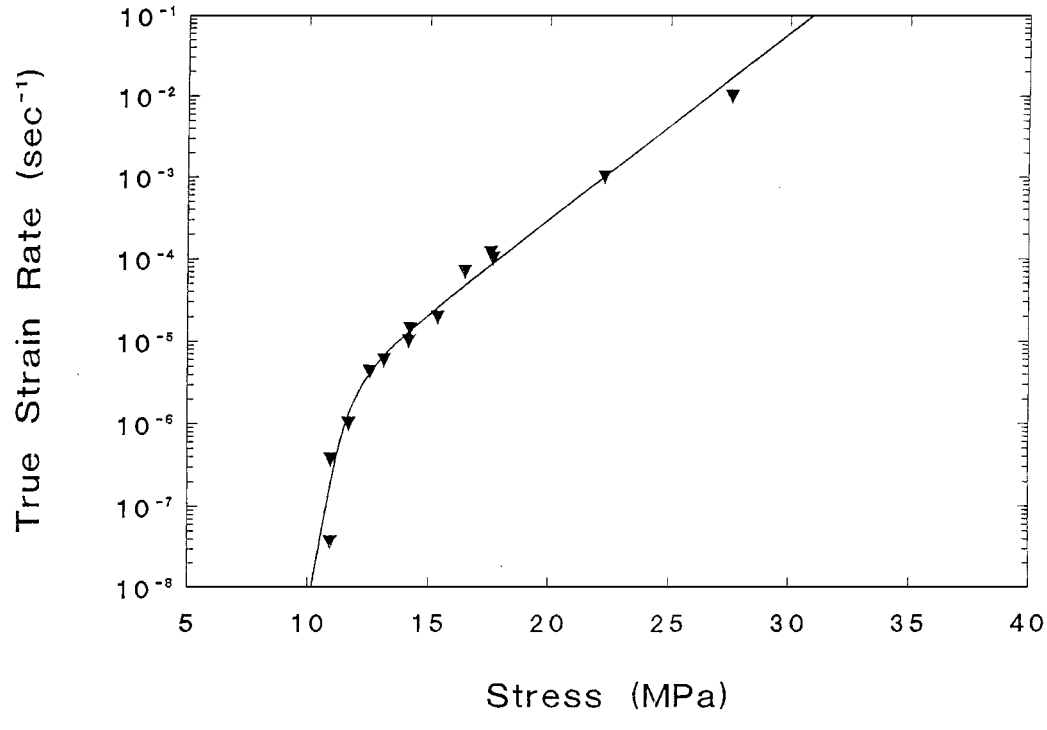

Figure 12 Eyring fits to the quenched morphology of grade C, — fit, ▼ experimental data.

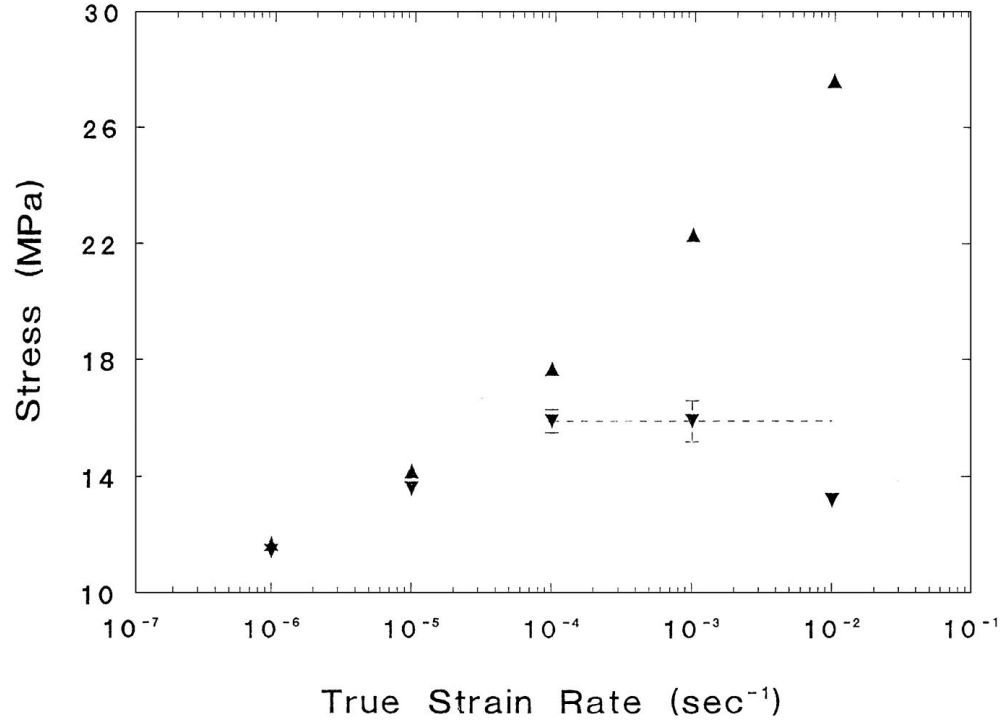

Figure 13 Recovery stress data for the quenched morphology of grade C at 20 °C, ▲ applied stress, ▼ recovery stress, --- plateau recovery stress (determined by averaging the recovery stresses at 10^{-3} and 10^{-4} s^{-1}).

describe the behaviour of the quenched morphology of material C. This model assumes that there is a single rate controlling process; several entities cross an energy barrier simultaneously to increase the strain of the material. In the strain rate range between the two yield points the model reduces to a spring (which carries the "recovery" stress), in parallel with a spring and dashpot (which carries the "effective" stress). To model the behaviour it is necessary to determine the effective stress acting upon the weak dashpot over a range of temperatures and strain rates. The temperatures used in this work were 20, 50 and 70 °C, and the recovery stress versus strain rate graphs are shown in Figs 13 to 15. The dotted lines represent estimated values of the recovery stress, since at high strain rates the cross head tends to overshoot the desired stop position, and the control algorithms on the electronics then cause it to oscillate up and down with decreasing amplitude until the desired stop position has been reached. This effect made the point at which the recovery stress equalled the test stress hard to detect. The resulting effective stress results are divided by the temperature at which they were obtained so that a unified plot of σ_e/T versus strain rate could be produced. The σ_e/T curves were then shifted horizontally by eye by differing amounts for each temperature, log a_T to give the best superposition and so produce a master curve, to which Equation 5, from [3], was fitted.

$$\sigma_e = \frac{2kT}{V^*} \sinh^{-1}\left(\frac{\dot{\varepsilon}}{K_T}\right)^{1/n} \tag{6}$$

Here σ_e is the effective stress, k is Boltzmann's constant, V^* is the activation volume, T is the temperature of the master curve, $\dot{\varepsilon}$ is the strain rate, K_T is a fitting constant and n is the average number of units making a simultaneous transition that increases the strain level of the material. The master curve and fitted curve are shown in Fig. 16. The amount by which the separate σ_e/T curves are shifted to produce the master curve allows us to derive an activation energy from the process from Equation 6 (from [3]).

$$\log a_T = \frac{nQ}{k}\left(\frac{1}{T} - \frac{1}{T_r}\right) \tag{7}$$

Where a_T is the shift factor for the curve, n and k are as above, Q is the activation energy and T and T_r are the temperature of the test data and the temperature of the master curve respectively.

The results obtained for fitting this model to the effective stress data determined from Figs 13 to 15, and with the value n constrained to be greater than 2 are shown in Fig. 16 and Table V, where they are compared to results from Brooks *et al*. (where n was also constrained to be greater than 2), and Fotheringham and Cherry. As can be seen the activation energies for materials B and C using this constraint are very similar, suggesting that the mechanism involved in both cases is the same. There is also reasonably good agreement between the values of n and K_T for: C from this work; B

TABLE V Comparison of results obtained by different workers on the quenched morphologies of three different materials using the Fotheringham and Cherry analysis

	C	B (Brooks)	LPE (F and C)
V^* (Å^3)	151	480	570
nQ (kJ mol^{-1})	38.5	51.5	—
n	2.34	3.24	3.1
Q (kJ mol^{-1})	16.4	15.9	—
K_T	0.2	0.2	0.127

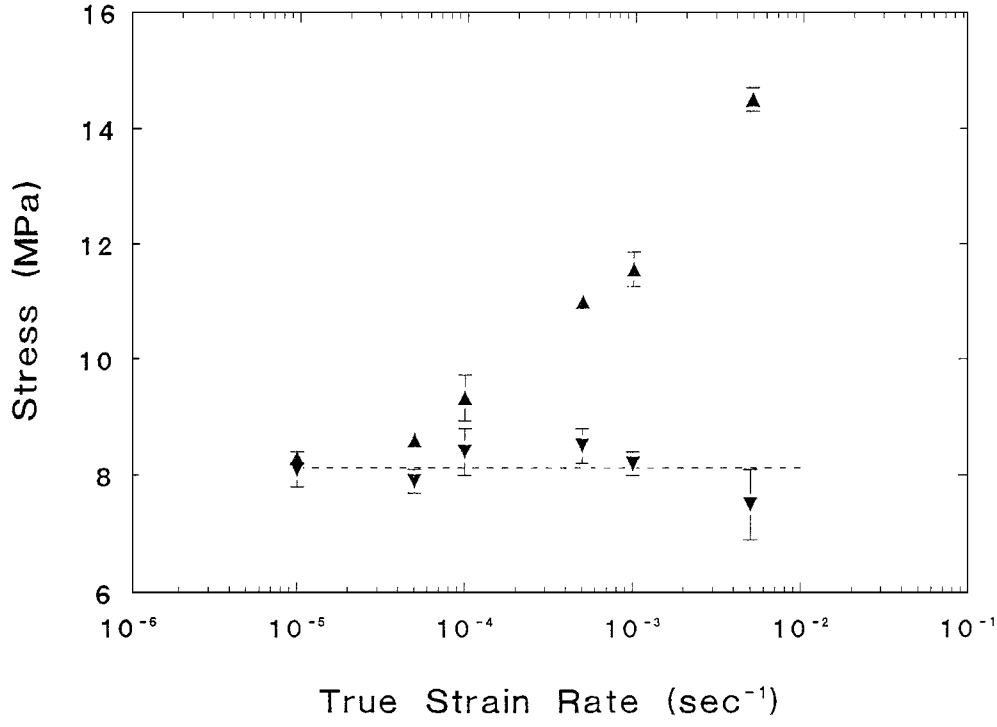

Figure 14 Recovery stress data for the quenched morphology of grade C at 50 °C, ▲ applied stress, ▼ recovery stress, --- plateau recovery stress (determined by averaging the recovery stress between 10^{-5} and 10^{-3} s^{-1}).

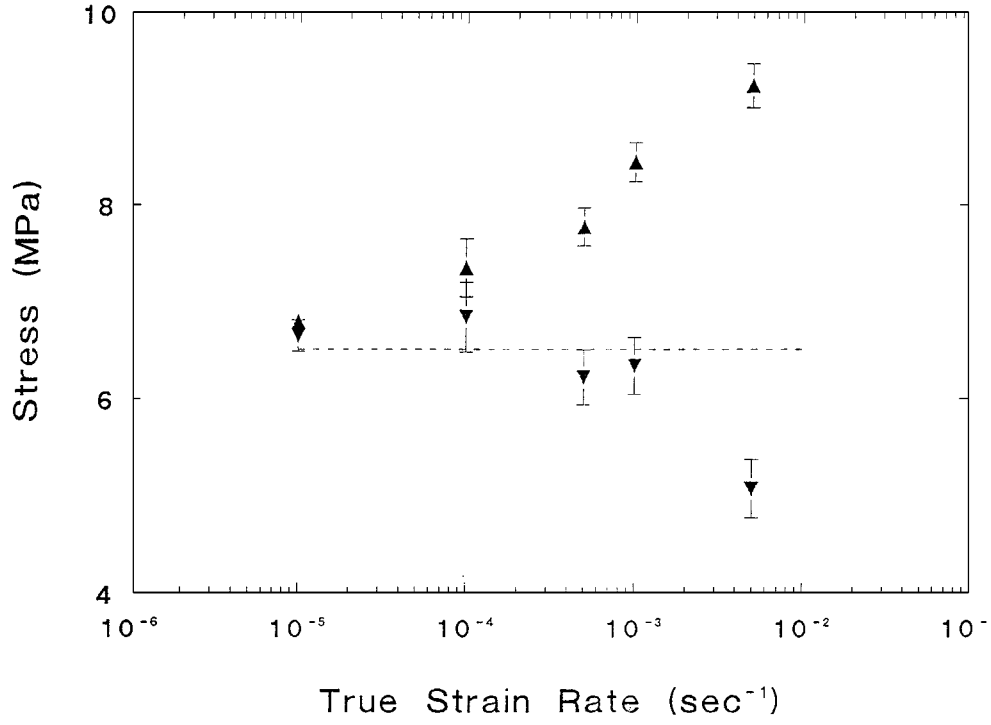

Figure 15 Recovery stress data for the quenched morphology of grade C at 70 °C, ▲ applied stress, ▼ recovery stress, --- plateau recovery stress (determined by averaging the recovery stress between 10^{-5} and 10^{-3} s^{-1}).

from Brooks; and a linear polyethylene from the work of Fotheringham and Cherry.

However this is not the only fit that can be achieved using this model.

If the constraint on the value of n is removed then the fit shown in Fig. 17 is achieved. As can be seen the parameters change markedly.

Also the "recovery" stress does not need to be based on the transient stress dip tests. Fig. 18 shows a fit achieved to the plateau creep data, but with a fixed "recovery" stress set arbitrarily at 8 MPa. This level was chosen because as stated earlier long term experiments had not detected any plateau creep at this stress level. Again the parameters are different.

All these fits were achieved by using a simple and unsophisticated least squares technique, where the sum of the differences between the calculated value and the actual value at each data point was minimised. All three fits seem equally valid in that they produce approximately the same value for the minimised sum, more extensive data and more sophisticated fitting procedures are needed to pursue this comparison further.

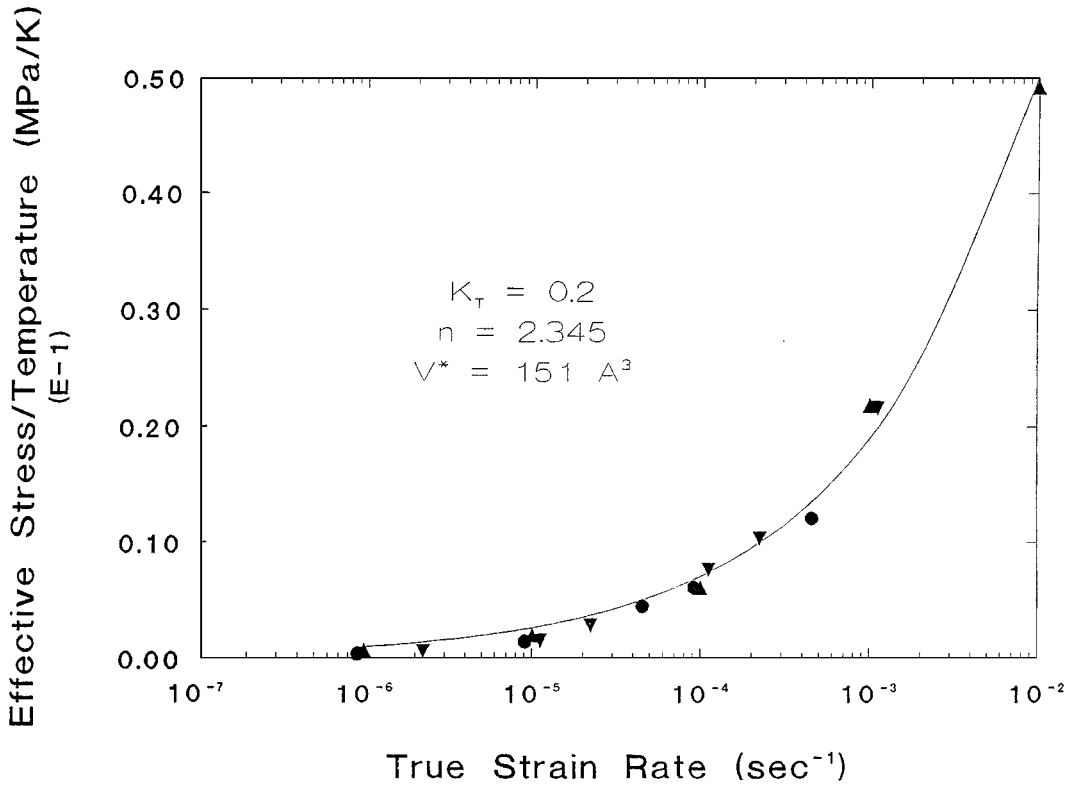

Figure 16 Master curve (referenced to 20 °C), and fitted curve (*n* constrained), for the Fotheringham and Cherry analysis for the quenched morphology of grade C, ▲ 20 °C, ▼ 50 °C, ● 70 °C, — fitted curve.

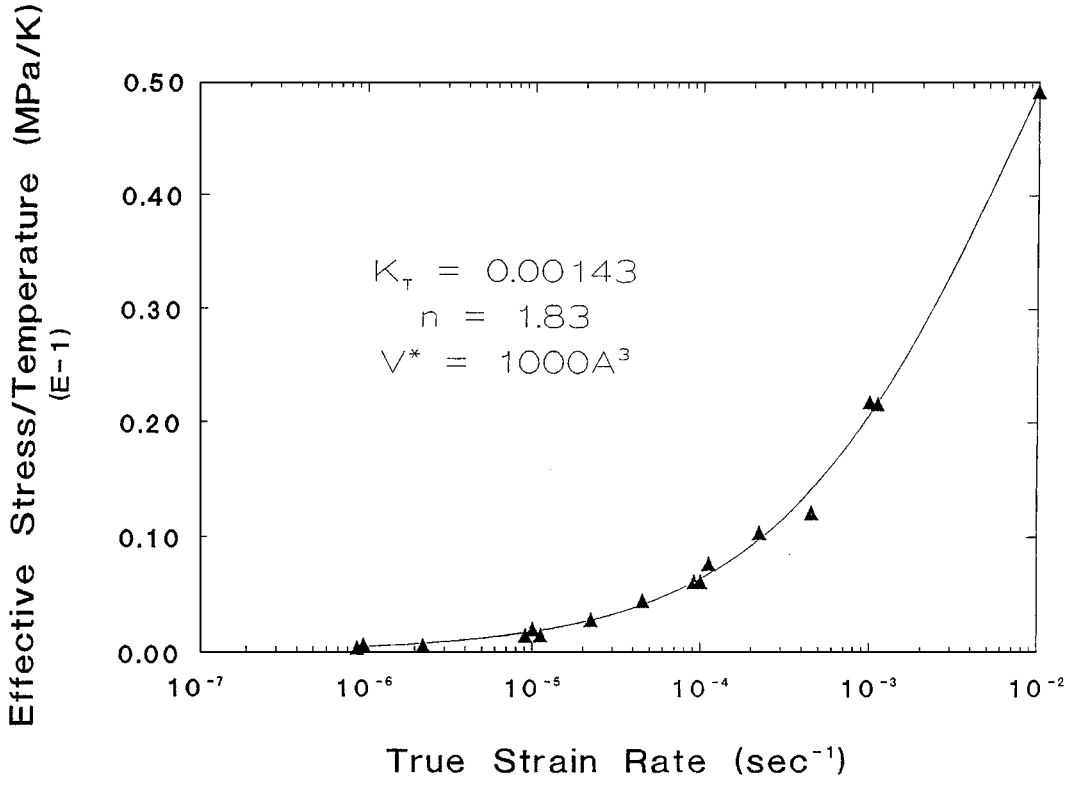

Figure 17 Master curve (referenced to 20 °C), and fitted curve (no constraint), for the Fotheringham and Cherry analysis for the quenched morphology of grade C, ▲ experimental data, — fitted curve.

5. Reconciling the differences between the two models

The existence of a unique relationship between stress, strain and strain rate would imply that both models could be used to describe the behaviour of the material, and hence we would expect relatively similar activation parameters from both approaches.

Whilst several fits are available for the Fotheringham and Cherry approach, the value of nQ is uniquely determined from the shift factor used to form the master

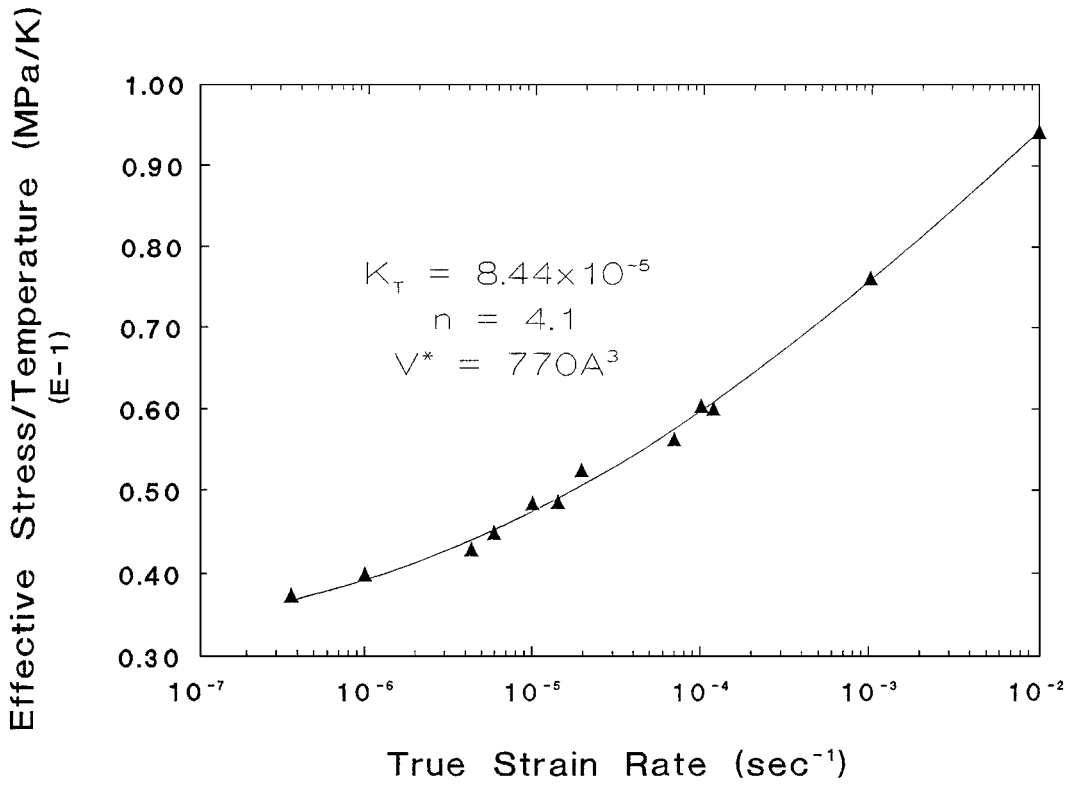

Figure 18 Master curve (referenced to 20 °C and containing both constant strain rate and plateau creep data at 20 and 50 °C), and fitted curve (recovery stress set at 8 MPa for both temperatures), with no constraint, for the Fotheringham and Cherry analysis for the quenched morphology of grade C, ▲ experimental data, — fitted curve.

curve. Hence the activation energy is always considerably less than the activation energy derived by the two process model. This low energy is not easy to interpret, whereas the activation energy derived from the two process model is in the region of the c-shear activation energy measured in dynamic/mechanical studies [12, 13].

The two process formulation also produces only one fit to the data, and does not require any constraints to used during fitting. Whilst the Fotheringham and Cherry model produces a good fit to the data, it is unsatisfactory that different ways of obtaining a quantitative fit produce very different values for the parameters involved. Although the transient stress dip approach provides very positive information regarding the yield behaviour, the fact that an arbitrarily chosen constant recovery stress can be chosen which still provides an acceptable fit shows its limitations.

Also, although it is not presented here, other work [10] has shown that the Fotheringham and Cherry approach will not describe the behaviour of the oriented material, whilst several authors [5, 6, 10] have shown that the two process model will quite successfully describe the behaviour of the oriented material.

Thus we must conclude that the two process model of Wilding and Ward is the better method of describing the behaviour of the behaviour of the isotropic material. The Fotheringham and Cherry approach is interesting, but is unsatisfactory in that the fitting parameters vary so considerably depending on what constraints are applied during fitting and how the recovery stress is defined.

6. Application of this work to real systems

There are several limitations of the work presented here that need to be expressly discussed.

Firstly we are dealing with uniaxial homogeneous tensile deformation only. It has not yet been established that a unique relationship exists between stress, strain and strain rate in other loading states (e.g. multi axial loading) and of course any such relationship would be expected to differ between loading states. Secondly it must also be stressed that the deformation is homogeneous; after the formation of a neck at the second yield point the deformation in the sample ceases to be homogeneous. The formation of a neck depends critically upon the local stress level in the material. The presence of flaws in the material, whether as defects in the edge of the sample formed during cutting or particulate inclusions, act as stress concentrators in the local region. Given the unique relationship between stress, strain and strain rate, the increased stress at a flaw will cause the local strain rate to be greater than the bulk strain rate of the sample, and hence the strain in the material at the flaw will reach the strain at which the second yield point occurs ahead of the rest of the material, and the neck will form at the flaw. By working in compression Brooks *et al*. [1] neatly avoided the problem with flaws, and hence reported higher strain values for the second yield point. It should be noted that during this work it was noticeable that the strain at which the second yield point occurred was seen to increase consistently for short periods immediately after the dumbbell cutter had been sharpened.

Finally although we know [10] that there is also a unique relationship between stress, strain and true strain rate in these materials in the fully oriented state (after complete propagation of the neck through the material), the activation volume derived from the two process model is radically different (of the order of 100 $Å^3$

for V_2 in material C). Thus any attempt to use this approach to model mathematically the transformation of the material from the isotropic state to the oriented state must at least take into account the dependence of the activation volume on the strain.

7. Conclusions

1. The slow cooled morphologies of the three grades studied have an increase in creep performance over the quenched morphologies which is directly proportional to the increase in yield stress.

2. There are two yield points in polyethylene, the first of which occurs at strains around 5% (which strain is relatively independent of the material), whilst the second occurs at strains of between 20 and 40% (depending on the material), and is associated with permanent plastic deformation. These two yield points are seen in both creep and constant strain rate tests.

3. There is evidence for the existence of a unique relationship between stress, strain and strain rate in the behaviour of grade C.

4. The two process (Eyring) model can be used to successfully model the behaviour of the quenched morphology of the isotropic grade C material, with an activation energy in the range quoted from dynamic mechanical data for the c-shear mechanism in polyethylene.

5. The two process model of Wilding and Ward is a more satisfactory model for describing the behaviour of the isotropic material than the Fotheringham and Cherry model, since the fits to the data which result are more robust.

Acknowledgements

The authors wish to acknowledge the help of Mr A. Channell, Mr L. Rose and Dr. G. Capaccio of BP Chemicals Ltd., Grangemouth. M. B. was jointly sponsored by BP Chemicals Ltd. and the E.P.S.R.C. as a C.A.S.E award Ph.D. student.

All materials used in this investigation were supplied in pellet form by BP Chemicals Ltd., Grangemouth.

References

1. N. W. BROOKS, R. A. DUCKETT and I. M. WARD, *Polymer* **33** (1992) 1872.
2. *Idem., J. Macromol. Sci.-Phys.* **B34** (1995) 29.
3. N. W. BROOKS, R. A. DUCKETT and I. M. WARD, *J. Rheology* **39** (1995) 29.
4. D. G. FOTHERINGHAM and R. W. CHERRY, *J. Mater. Sci.* **13** (1978) 951.
5. M. A. WILDING and I. M. WARD, *Polymer* **22** (1981) 870.
6. *Idem., ibid.* **19** (1978) 969.
7. O. D. SHERBY and J. E. DORN, *J. Mech. Phys. Solids* **19** (1956) 165.
8. P. D. COATES and I. M. WARD, *J. Mater. Sci.* **13** (1978) 629.
9. P. D. COATES, A. G. GIBSON and I. M. WARD, *ibid.* **15** (1980) 359.
10. M. BONNER, PhD thesis, University of Leeds, 1995.
11. H. J. EYRING, *Chem. Phys.* **4** (1936) 283.
12. N. ALBEROLA, J. Y. CAVAILLE and J. PEREZ, *J. Polym. Sci. B* **28** (1990) 569.
13. T. KAJIYAMA, T. OKADA, A. SAKODA and M. TAKAYANAGI, *J. Macromol. Sci.-Phys.* **B3** (1973) 583.

Received 16 June 1997
and accepted 10 November 1998